Nucleic Acids Research, 2025, **53**, gkaf1290
https://doi.org/10.1093/nar/gkaf1290
Synthetic Biology and Bioengineering

Metabolite-responsive scaffold RNAs for dynamic CRISPR transcriptional regulation

Anthony M. Stohr, Helena Hansen, Blake Richards, Hayeon Park, Antonio G. Goncalves, Ayushi Agrawal, Mark Blenner*, Wilfred Chen*

Department of Chemical and Biomolecular Engineering, University of Delaware, Newark, DE 19716,United States

*To whom correspondence should be addressed. Email: blenner@udel.edu
Correspondence may also be addressed to Wilfred Chen. Email: wilfred@udel.edu

Abstract

CRISPR activation is a powerful tool to upregulate a vast array of genes in many different contexts. However, there are few dynamic CRISPR transcriptional programs, which limit its usage in the creation of living biosensors, self-regulating microbial factories, or conditional therapeutics. Here, we address this limitation by embedding a molecular switch directly into a guide RNA to create a combined sensor–actuator called a metabolite-responsive scaffold RNA (MR-scRNA). We demonstrate the regulatory potential for MR-scRNAs by conditionally activating genes in three different kingdoms of life. We create MR-scRNAs responsive to two distinct metabolites, theophylline and tryptophan, by swapping the molecular switch used. MR-scRNAs respond quickly in a dose-dependent manner specifically to their target metabolite and enhance biochemical production when used as a dynamic regulator of pathway enzyme expression. The broad functionality and ease of design of the MR-scRNAs offer a promising tool for dynamic cellular regulation.

Graphical abstract

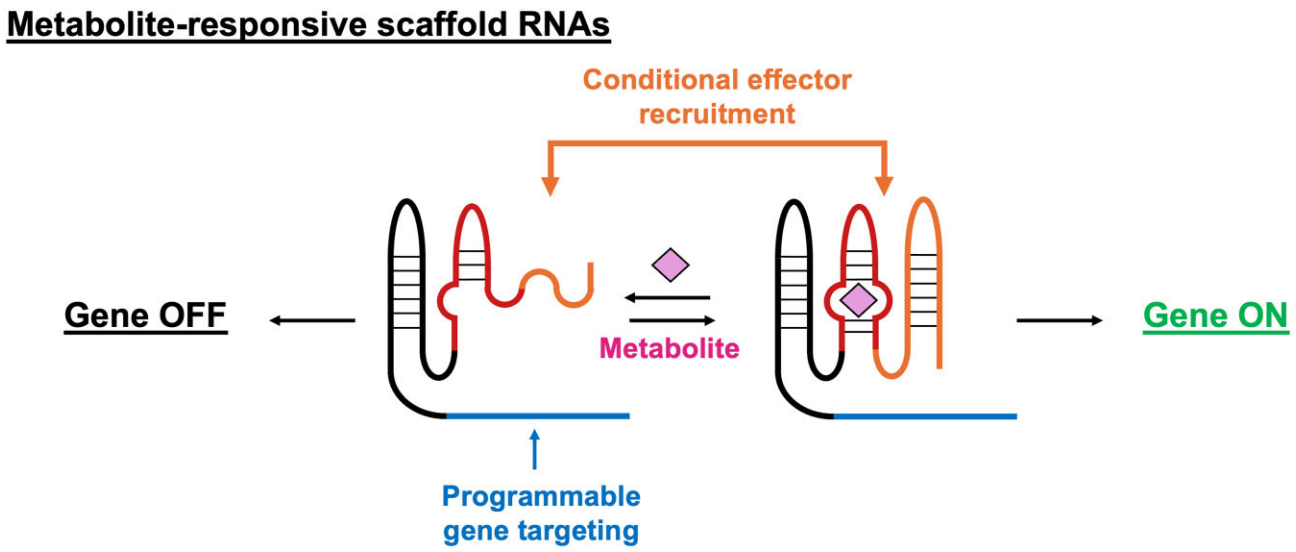

Introduction

Synthetic biology and metabolic engineering have converted microbes into living factories that can upcycle simple feedstocks into commodity chemicals, complex natural products, and therapeutics [1–4]. Maximizing cellular productivity, titer, and yield requires that the expression of both native metabolic pathways and heterologous enzymes must be finely controlled in concert. Traditional approaches toward balancing metabolic flux rely on static optimization of pathway enzyme expression through screening promoter or ribosome binding site libraries to modulate expression of each gene combinatorially or to knock out competing pathways [5–7]. However, static gene regulation does not take into account that cellular environments vary significantly throughout the cell life cycle, leading to mismanagement of resources and thus suboptimal performance. Conversely, dynamic reg-

Received: July 27, 2025. **Revised:** October 16, 2025. **Accepted:** October 17, 2025

ulatory strategies aim to balance the competing demands of the cell by cycling between growth and production states [8–12]. Ideally, this is achieved by allowing the cell to interpret important physiological cues, such as branch point metabolite concentrations, to modulate the expression of production enzymes for better allocation of cellular resources and improved product titers [10].

CRISPR–Cas transcriptional regulation systems are a promising method for precise control of gene expression. Programmable targeting of either the CRISPR activation (CRISPRa) or repression (CRISPRi) complex to the gene of interest is enabled by complementary base pairing of the spacer sequence to the target locus [13]. Gene targets can be changed simply by exchanging the spacer sequence, and simultaneous gene activation and repression of multiple genes is possible using multiple single guide RNAs (sgRNAs). Both types of CRISPR transcriptional control systems are effective in bacterial [14–17], fungal [18, 19], and mammalian [13, 18, 20] hosts, demonstrating the broad generalizability of these gene expression schemes. However, one primary limitation is that most CRISPR-based gene control systems are static in nature. While there are several recent examples of input-responsive CRISPR transcriptional control systems [19–22], these schemes rely on a limited set of chemically induced protein–protein interactions [23] that respond to a small number of chemicals that must be exogenously supplied, such as rapamycin, abscisic acid, and gibberellin, or light-controlled systems that are impractical at scale. Conversely, RNA aptamers can be readily generated to selectively bind to a diverse array of molecules [24–27] and directly incorporated into the sgRNA to minimize the number of components required for dynamic cellular regulation [28–31]. However, existing small-molecule-responsive sgRNA designs are limited by the range of hosts that they are functional in, the reversibility of their regulatory mechanism, and their ability to regulate transcriptional activation.

To design a generalizable dynamic regulatory strategy for metabolite-responsive CRISPR transcriptional control, we exploited a class of highly efficient self-contained RNA switches that link the binding of a chemical input to the binding of a protein target [32]. These RNA switches conditionally form an MS2 bacteriophage coat protein (MCP)-binding hairpin only when the metabolite of interest binds to its cognate aptamer (Fig. 1A). Conveniently, in one version of CRISPRa, the transcriptional activator is translationally fused to MCP and constitutively recruited to the MS2 aptamer located on the 3′ end of the scaffold sgRNA (scRNA) [14, 15, 18]. By replacing this static hairpin with RNA switches, we designed metabolite-responsive scaffold RNAs (MR-scRNAs) that enabled conditional CRISPRa in both prokaryotic (*Escherichia coli*) and eukaryotic cells (*Saccharomyces cerevisiae* and HEK239T) (Fig. 1B). We demonstrated that MR-scRNAs exhibit dose-dependent behavior and are highly specific to the target metabolite, and the metabolite-sensing RNA aptamer can be swapped to respond to alternative ligands. Using a tryptophan MR-scRNA, we dynamically regulated the expression of the multi-gene violacein biosynthesis pathway, leading to 10-fold improved product titers and increased strain stability. We envision that the generalizable functionality of the MR-scRNA will provide new opportunities for biosensing and dynamic cellular regulation.

Materials and methods

Plasmid construction

Plasmids used in this study are listed in Supplementary Table S1. The sequences of each MR-scRNA and scRNA used in this study are reported in Supplementary Table S2. Complete plasmid sequences are available from our publicly accessible Benchling repository, and relevant plasmids are available from Addgene.

Plasmids were constructed using standard molecular cloning techniques and sequence verified. Bacterial CRISPRa plasmids were derived from Addgene plasmids 153025 (a gift from Jesse Zalatan) [15], 192640 (a gift from Jesse Zalatan) [33], and 206802 (a gift from James Carothers) [21]. Yeast CRISPRa plasmids were derived from Addgene plasmids 62313 and 62283 (gifts from Wendell Lim and Stanley Qi) [18]. Mammalian CRISPRa plasmids were derived from Addgene plasmid 84239 (a gift from Stanley Qi) [20] or a commercial pcDNA3.1 vector. Violacein biosynthesis genes were obtained from Addgene plasmid 73440 (a gift from Mattheos Koffas) [34].

MR-scRNA characterization in *E. coli*

Escherichia coli strain MG1655 was transformed with the specified CRISPRa and reporter plasmids. Freshly transformed cells were inoculated in LB media (10 g/l tryptone, 5 g/l yeast extract, and 10 g/l tryptone) containing 100 μg/ml carbenicillin and 30 μg/ml chloramphenicol and grown overnight at 37°C with agitation. Cells were subcultured (1:100 dilution) into fresh media supplemented with the specified theophylline (or caffeine) concentration and grown for 8–12 h at 37°C with agitation prior to measurement. In the case of metabolite cycling experiments, cells were measured and subcultured (1:100 dilution) every 6 h into fresh media with or without 1 mM theophylline. A 100 μl sample of each culture was collected, and the OD_{600} and mRFP1 fluorescence (excitation, 540 nm; emission, 600 nm; bandwidth, 13.5 nm) of each were measured in a BioTek Synergy H4 plate reader.

MR-scRNA response kinetics in *E. coli*

Cells were transformed and grown as described in the previous section. Cells were subcultured (1:100 dilution) into fresh media supplemented with (for off-rate kinetics) or without (for on-rate kinetics) 1 mM theophylline and grown for 6 h at 37°C with agitation. Cells were then further subcultured (1:100 dilution) into fresh media with (for on-rate kinetics) or without (for off-rate kinetics) 1 mM theophylline. At each specified time point, 10 μl of cells were collected and diluted into 90 μl of phosphate buffered saline (PBS) buffer for flow cytometry analysis.

An ACEA NovoCyte Flow Cytometer was used to analyze 10 000 single cells per sample. Events were first gated on forward scatter height versus side scatter height to determine the population of cells and then gated on forward scatter height versus area to determine the population of single cells. The PE-Cy5 channel was used to measure the fluorescence intensity of mRFP1. An example gating strategy and histogram are depicted in Supplementary Fig. S16.

Tryptophan MR-scRNA characterization in *E. coli*

Cells were transformed as described previously. Cells were initially cultured in the standard MOPS EZ rich defined media

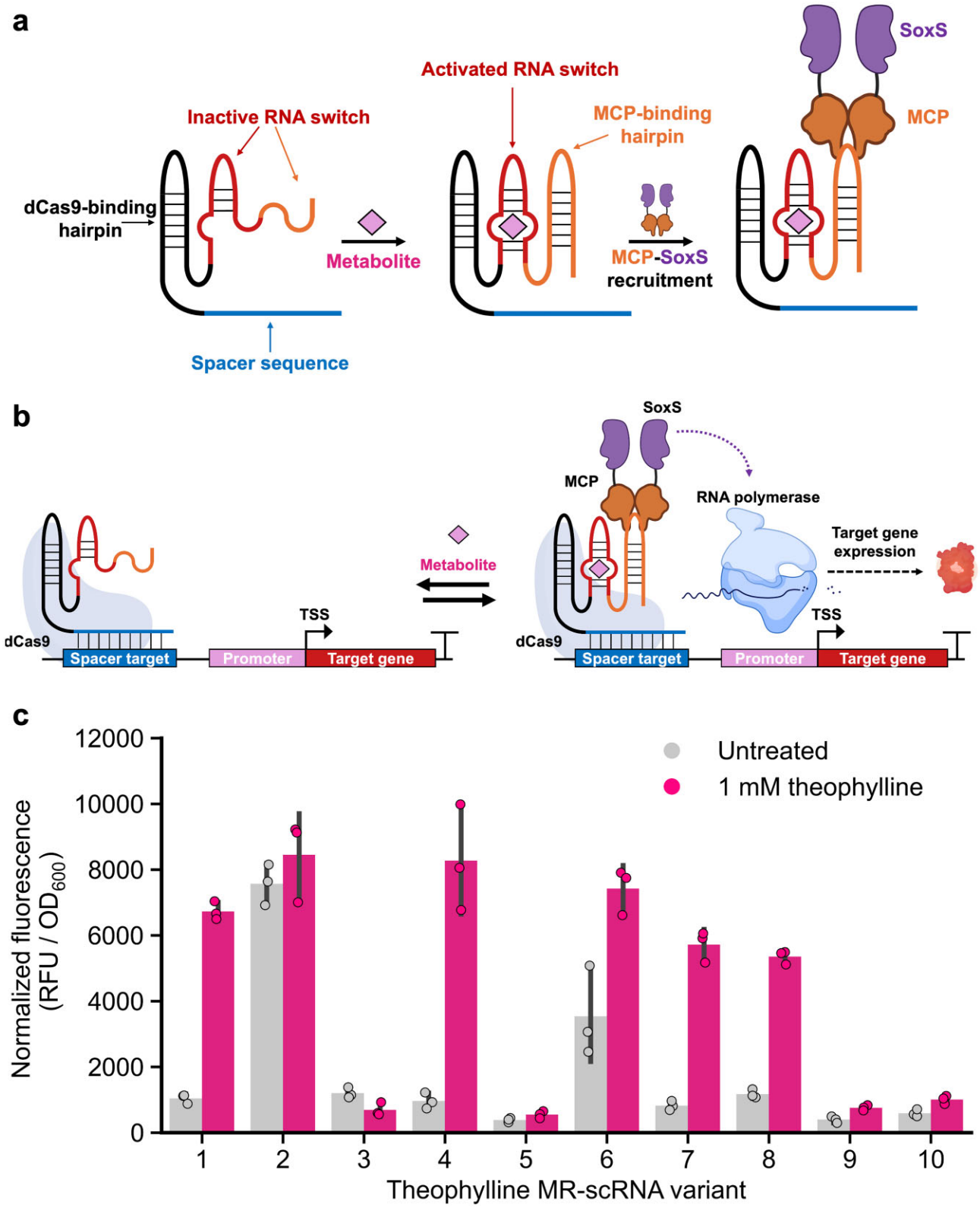

Figure 1. Design of metabolite-responsive scRNAs for conditional gene activation. (**A**) The MR-scRNA consists of an unstructured spacer sequence complementary to the genetic target, a dCas9-binding hairpin, and an RNA switch that undergoes a conformational shift once bound to the target metabolite to form an MCP-binding hairpin. In the active state, the MR-scRNA can bind to MCP-SoxS transcriptional activator and induce gene activation. (**B**) Design schematic of the metabolite-responsive CRISPRa system. If the metabolite of interest is not present, the MR-scRNA–dCas9 complex is localized upstream of the target gene, but the inactive MR-scRNA does not recruit the MCP-SoxS transcriptional activator. However, in the presence of the target metabolite, the activated MR-scRNA binds to the MCP-SoxS transcriptional activator, which in turn recruits the RNA polymerase and induces expression of the target gene. (**C**) Screening for functional MR-scRNAs in E. coli that conditionally activate mRFP1 expression in response to their target metabolite, theophylline. The full sequences of each MR-scRNA variant can be found in Supplementary Table S2. All values are mean ± s.d. of $n = 3$ biological replicates. Abbreviations: TSS, transcription start site; RFU, relative fluorescent units; OD_{600}, optical density at 600 nm.

formulation (Teknova) containing 100 μg/ml carbenicillin and 30 μg/ml chloramphenicol and grown overnight at 37°C with agitation. Cells were subcultured (1:100 dilution) into fresh MOPS EZ rich defined media formulated without tryptophan, so that tryptophan could be supplemented at the specified concentrations. Cells were grown for 8 h at 37°C with agitation. Cells were collected and analyzed by plate reader or flow cytometry as described in the previous sections.

Violacein biosynthesis and quantification

Escherichia coli strain MG1655 was transformed with the specified CRISPRa and biosynthesis plasmids. Freshly transformed cells were inoculated in LB media containing 100 μg/ml carbenicillin and 30 μg/ml chloramphenicol and grown for 8 h at 37°C with agitation. Cells were subcultured (1:100 dilution) into shake flasks containing 25 ml of fresh media and any specified metabolites and grown for 8 h at 30°C with agitation.

Violacein was harvested and quantified as previously described [34]. Briefly, a 500 μl sample was collected from each culture, and cells were harvested by centrifugation at 5000 rcf for 5 min. After removing the supernatant, cells were boiled in 600 μl of methanol containing 1% (v/v) acetic acid for 5 min. Cellular debris was removed by centrifugation at 21 000 rcf for 10 min, and extracts were filtered. Violacein quantification was performed on an Agilent 1290 Infinity II HPLC system with a Waters C18 column (WAT086344, 150 mm × 3.9 mm, 4 μm particle size). The solvent gradient was as described previously [34], with an injection volume of 10 μl. Violacein was detected at 6.3 min with a diode-array detector at 565 nm.

MR-scRNA characterization in yeast

To generate a yeast strain with galactose-inducible CRISPRa machinery, the *S. cerevisiae* reporter strain W303 *TRP1*::pTET07-Venus (a gift from Jesse Zalatan) [19] was transformed with pSC-CRISPRa integration vector linearized by digestion with SfiI. The resulting yeast cells were transformed with the specified scRNA plasmids. Isolated colonies were inoculated in yeast synthetic complete media deficient in uracil (YSC-URA) supplemented with 20 g/l glucose and grown overnight at 30°C with agitation. To relieve carbon catabolite repression, cells were diluted to an OD of 0.5 into fresh media containing 20 g/l raffinose and grown overnight at 30°C with agitation. Cells were again diluted to an OD of 0.5 into fresh media containing 20 g/l raffinose, 0.01% (w/v) galactose, and theophylline or tryptophan as specified and grown overnight at 30°C with agitation. Cells were harvested by centrifugation and washed in PBS buffer. The OD_{600} and fluorescence (excitation, 500 nm; emission, 530 nm; bandpass filter, 9 nm) of 100 μl of resuspended cells were measured in a BioTek Synergy H4 plate reader.

MR-scRNA characterization in human cells

HEK293T pTRE3G–dscGFP (a gift from Stanley Qi) [18, 20, 35] cells were cultured in Dulbecco's modified Eagle medium with high glucose, sodium pyruvate, and GlutaMAX (Gibco) supplemented with 1× penicillin–streptomycin and 10% (v/v) fetal bovine serum. Cells were maintained at confluency below 80%–90% at 37°C and 5% CO_2. For each experiment, cells were seeded at a density of either 10 000 or 50 000 cells per well in 96-well or 24-well tissue culture treated-plates, respectively, and transfected 24 h after seeding. Cells were transfected with a total of 50 or 250 ng of DNA in 96-well or 24-well plate experiments, respectively. Transfections were prepared by combining dCas9, gRNA, and MCP-VPR plasmids in a 4:5:1 mass ratio using the vendor's recommended ratio of jetOPTIMUS (Polyplus) transfection reagent (1 μg DNA:1 μl reagent). Cells were induced 24 h after transfection by adding 100 mM theophylline solution prepared in 60 mM sodium hydroxide (to improve solubility) as specified to the culture media. Cells were washed in PBS, trypsinized, and harvested for flow cytometry analysis 24 h after induction.

An ACEA NovoCyte Flow Cytometer was used to analyze 10 000 transfected cells per sample. Events were first gated on forward scatter height versus side scatter height to determine the population of cells and then gated on forward scatter height versus area to determine the population of single cells. Cells were then gated with the PE-Cy5 channel to identify transfected cells (each gRNA expression plasmid contains a mCherry reporter). The FITC channel was used to measure the fluorescence intensity of dscGFP. An example gating strategy and histogram is depicted in Supplementary Fig. S17.

Endogenous gene activation

HEK293T cells (ATCC CRL-3216) were cultured and maintained as described in the previous section. Cells were seeded, transfected, and induced in 24-well plates as described in the previous section. Cells were washed in PBS, trypsinized, and harvested 24 h after induction. Cell pellets were harvested by centrifugation at 400 rcf for 5 min and stored frozen at −80°C prior to extraction. Frozen cell pellets were thawed and resuspended in 600 μl of Monarch StabiLyse DNA/RNA buffer. RNA was extracted from lysed cell pellets and DNase treated using the Monarch Spin RNA Isolation Kit (Mini) (NEB). Purified RNA samples were eluted in nuclease-free water, and their concentration and quality were assessed using a NanoDrop 2000 (Thermo Scientific). RT-qPCR was performed on 200 ng of total RNA with a Bio-Rad CFX96 Real-Time System using the Luna Universal One-Step RT-qPCR kit (NEB). Each biological replicate was analyzed in duplicate technical reactions, and the resulting Cq values were averaged. Target gene expression was normalized to *GAPDH* mRNA levels and compared against cells transfected with a non-targeting MR-scRNA using the ΔΔCq method [36]. Oligonucleotides used for RT-qPCR are listed in Supplementary Table S3.

Statistical analysis

All data in the study are displayed as the mean ± standard deviation of three biological replicates along with the measurements of individual replicates unless otherwise indicated. Statistical significance was assessed at $P \leq .01$ with the one-tailed Welch's *t*-test. All data figures and statistical analysis were prepared in Python 3.8.8 using matplotlib, seaborn, pandas, and SciPy libraries.

Results

Metabolite-responsive scaffold RNAs conditionally activate gene expression

To develop a metabolite-responsive CRISPRa system, we created a metabolite-responsive scaffold RNA (MR-scRNA) that conditionally recruits a transcriptional activator, SoxS, to the target gene in *E. coli* (Fig. 1A). The MR-scRNA con-

sists of three functional moieties: a spacer sequence encoding the genetic target, a dCas9-binding hairpin, and a 3′ metabolite-responsive RNA switch. The RNA switch undergoes a conformational shift upon metabolite binding that enables the formation of an MCP-binding hairpin. As with the static CRISPRa system, this motif is used to recruit an MCP-activation domain fusion protein to the CRISPR complex and initiate transcription of the target gene (Fig. 1B).

As a proof of concept, we selected the 10 best-performing theophylline-responsive RNA switches previously characterized by an *in vitro* high-throughput screen [32] and inserted each in place of the static MCP-binding hairpin present in the original scRNA to create a set of theophylline MR-scRNAs. Theophylline was chosen as a model metabolite for our initial screens because it is not endogenously produced or consumed, and its cognate aptamer is well studied [37]. We examined MR-scRNA activity by targeting an engineered minimal promoter upstream of a monomeric red fluorescent reporter (mRFP1) [21] in *E. coli* in the presence and absence of theophylline (Fig. 1C). Six of the 10 theophylline MR-scRNA designs screened had a significant increase in mRFP1 expression when cells were treated with theophylline, with three MR-scRNAs producing a greater than five-fold response to the target metabolite. Of the four non-responsive MR-scRNAs, two variants had minimal CRISPRa activity, while two variants were constitutively active. We confirmed that the addition of theophylline had no significant impact on CRISPR-mediated gene activation when the static scRNA design is used (Supplementary Fig. S1), confirming that the metabolite-responsive RNA switch is required for the conditional activation of the reporter gene.

We compared the metabolite-induced response of the RNA switches in their previously studied context (conditional MCP-binding *in vitro*) [32] and in our study (conditional gene activation) and found no correlation (Supplementary Fig. S2). This is unsurprising, as the requirements for CRISPR-mediated gene activation are more stringent than those of simply binding to MCP. For the MR-scRNA to correctly induce expression, both the dCas9-binding motif and RNA switches must fold properly while maintaining an unstructured spacer region for hybridization to the target site. Additionally, there are strict requirements for the spatial orientation and distance of the MCP-SoxS activator that significantly reduce gene activation if not met [14, 15].

MR-scRNA sensitivity, specificity, and response dynamics

We further characterized the ability of the theophylline MR-scRNA to conditionally regulate gene activation in *E. coli*. We selected variant #1 for subsequent analysis due to its high fold response and minimal variance compared to other designs. We first titrated cells with different theophylline concentrations to determine whether the MR-scRNA response is dose-dependent. We observed a linear response to theophylline concentrations between 100 and 2 500 μM (Fig. 2A). Metabolite-induced gene activation continued to occur at theophylline concentrations >2500 μM, but at these concentrations cells exhibited significant toxicity, consistent with other reports in the literature (Supplementary Fig. S3) [38, 39]. The maximal and basal activation of the conditional output response could also be modulated by copy number variation of the target gene (Supplementary Fig. S4).

Highly specific target recognition is critical for intracellular biosensors and regulators due to the abundance of molecules with similar size, shape, and charge present in the cellular environment. Minimal cross-reactivity with structurally similar molecules is particularly important in the context of metabolic engineering as many metabolites within a biosynthetic pathway can differ by only a single functional group. Aptamers are known for being highly specific to the target ligand, with exceptional discrimination against structurally similar molecules [37, 40]. We evaluated the specificity of the theophylline MR-scRNA for its cognate metabolite against caffeine. Similar to theophylline, caffeine is also a methylxanthine, but it contains an additional methyl group present at the N7 position (Fig. 2B). Cells treated with caffeine exhibited a similar toxicity profile to those treated with theophylline (Supplementary Fig. S3), but unlike those stimulated by theophylline treatment, the MR-scRNA did not activate reporter expression in response to caffeine (Fig. 2B and Supplementary Fig. S5).

We next examined the kinetics and dynamics of the MR-scRNA induction in response to the target metabolite. To determine the on- and off-rate kinetics of metabolite-responsive CRISPRa, we first cultured cells with or without 1 mM theophylline for 6 h to induce the expected cell state ("on" if treated with theophylline or "off" if untreated) and then diluted cells into fresh media corresponding to the opposite state. We measured fluorescence by flow cytometry over time; cells were measured just prior to and for 4 h after media exchange (Fig. 2C). In both cases, a significant change in mRFP1 levels was observed within 1 h after metabolite addition or removal. While the RNA switches embedded within the MR-scRNA previously exhibited binding or unbinding on much shorter timescales (seconds to minutes) [32], changes of detectable mRFP1 signal are limited by the rates of transcription, translation, and chromophore maturation [41]. To demonstrate the potential usefulness of MR-scRNAs as dynamic regulators, we also repeatedly transferred cells between media with or without theophylline and found that the cells cycled between the on- and off-states in response to the target ligand as expected (Fig. 2D). Additionally, we observed that the MR-scRNA generated a population-wide response, with ∼90% of the treated cells exhibiting a detectable response to theophylline stimulation (Supplementary Fig. S6).

MR-scRNAs modulate gene expression in eukaryotes

As part of our goal to develop a generalizable metabolite-responsive transcriptional control platform, we tested the ability of the MR-scRNAs to conditionally activate genes in eukaryotic cells. We ported the MR-scRNA into the framework necessary for CRISPR activation in yeast and human cells (Fig. 3A). The only modifications required were to add nuclear localization signaling peptides to the protein components and swap the bacterial transcriptional activator, SoxS, with one compatible for gene activation in eukaryotes, VP64-p65-Rta (VPR) [42]. Other than replacing the spacer sequences, we made no changes to the MR-scRNA designs.

To test whether the MR-scRNA is functional in yeast, we transformed plasmids expressing a constitutively active scRNA, a non-targeting scRNA, or a theophylline-responsive MR-scRNA into an *S. cerevisiae* reporter cell line [18, 19] with a Venus fluorescent reporter and the CRISPRa machinery

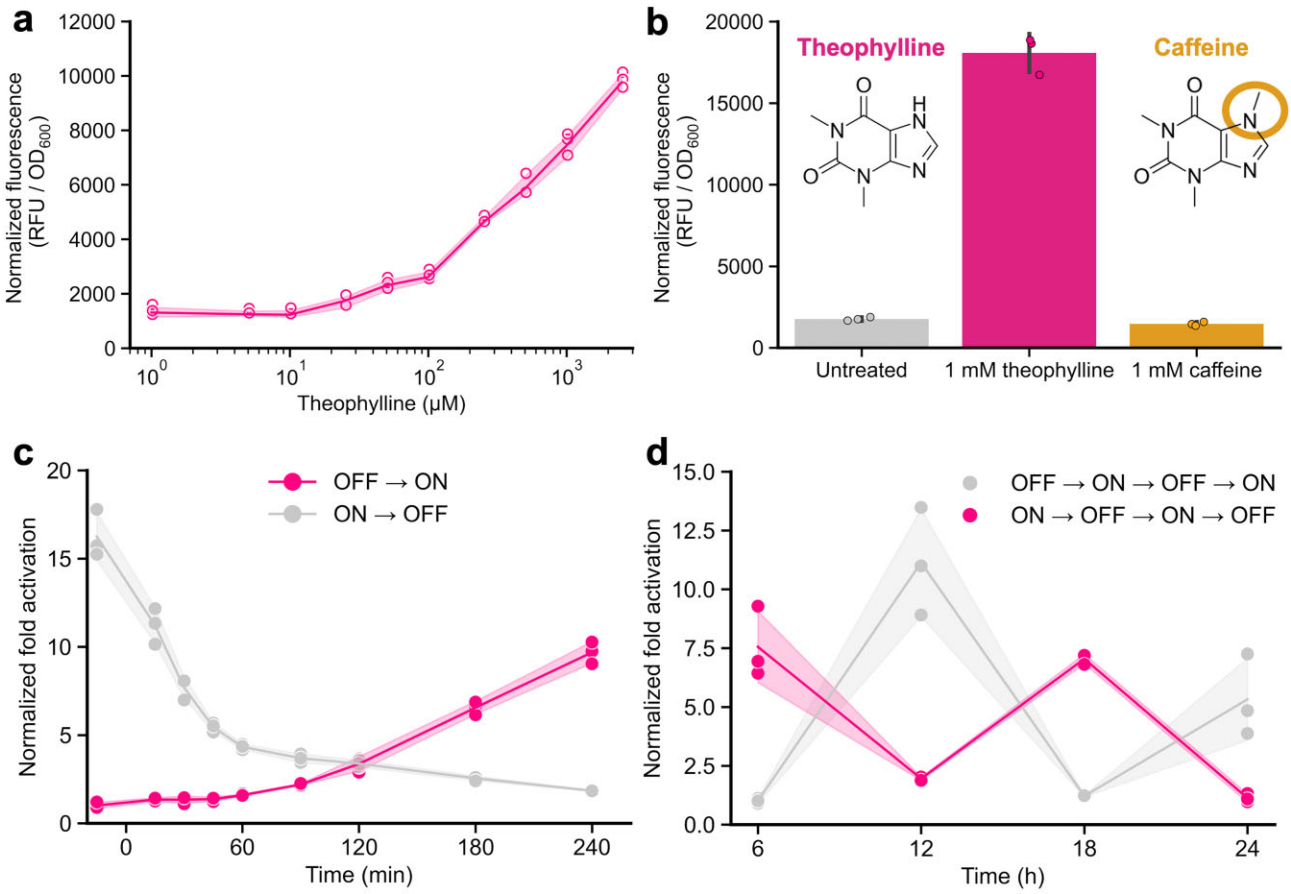

Figure 2. Theophylline MR-scRNA response characterization. (**A**) Dose–response curve of the theophylline MR-scRNA in response to the target metabolite. (**B**) The theophylline MR-scRNA can differentiate between the target metabolite and a structurally similar compound, caffeine. The chemical structures for each compound are shown; the additional methyl group present within caffeine is highlighted. (C, D) Response kinetics and dynamics of the theophylline MR-scRNA system when either untreated (OFF state) or treated with 1 mM theophylline (ON state). Gene activation was normalized by the average normalized fluorescence of three biological controls without 0 mM theophylline treatment at each time point. (**C**) Response kinetics of the MR-scRNA system after passage into fresh media at 0 min. (**D**) Response dynamics of the MR-scRNA system after repeated passaging into fresh media every 6 h. All values are mean ± s.d. of n = 3 biological replicates; shaded regions in panels (A), (C), and (D) represent the s.d. Abbreviations: RFU, relative fluorescent units; OD600, optical density at 600 nm.

(dCas9 and MCP-VPR) integrated in the genome. Metabolite-responsive gene activation was only observed in yeast cells expressing the MR-scRNA (Fig. 3B). The MR-scRNA increased mVenus expression 18.5-fold in response to theophylline. However, the activated state was only 26% of the maximal gene expression achieved by the static scRNA design; similar to the bacterial application, this is likely due to reduced affinity of the RNA switch for MCP relative to the constitutively formed MS2 aptamer. Similarly, we assessed whether MR-scRNAs could conditionally drive gene activation in mammalian cells. We transfected plasmids expressing dCas9, MCP-VPR, and either an scRNA control or a theophylline-responsive MR-scRNA into a HEK239T reporter cell line previously engineered to express GFP from a minimal promoter [18, 20, 35]. As with yeast, only HEK239T cells expressing the MR-scRNA demonstrated increased reporter expression after theophylline treatment (Fig. 3C). We observed a dose-dependent response by the MR-scRNA to the target ligand over similar concentration ranges as in *E. coli* (Supplementary Fig. S7). We attempted to improve MR-scRNA activity in human cells by adding an additional tracr terminator hairpin that previously increased gene activation in eukaryotes [14, 18], but this modification completely abolished all activity likely due to disruptions to the functional motifs within the adjacent RNA switch (Supplementary Fig. S8).

The similar performance of MR-scRNA across three distinct host organisms was surprising, as RNA devices are heavily influenced by temperature differences [43–45] and magnesium concentrations [46, 47], which vary significantly across each host. For instance, both temperatures used to test MR-scRNAs in cells (37°C for bacteria and mammals versus 30°C for yeast) differed from the initial *in vitro* screening conditions for the RNA switches (24°C) [32]. Additionally, cytosolic magnesium levels can drastically differ between the bacterial and mammalian cells [48, 49] and are less than those used to screen for the RNA switches (4 mM) [32]. Together, these results indicate that the MR-scRNA and the corresponding RNA switches are functional in a broad range of environments and applications.

MR-scRNAs regulate endogenous gene expression

A key advantage of CRISPR regulation over other transcriptional control systems is the ability to programmably target genes without the need for promoter editing or engineering [42, 50]. We tested whether MR-scRNAs could con-

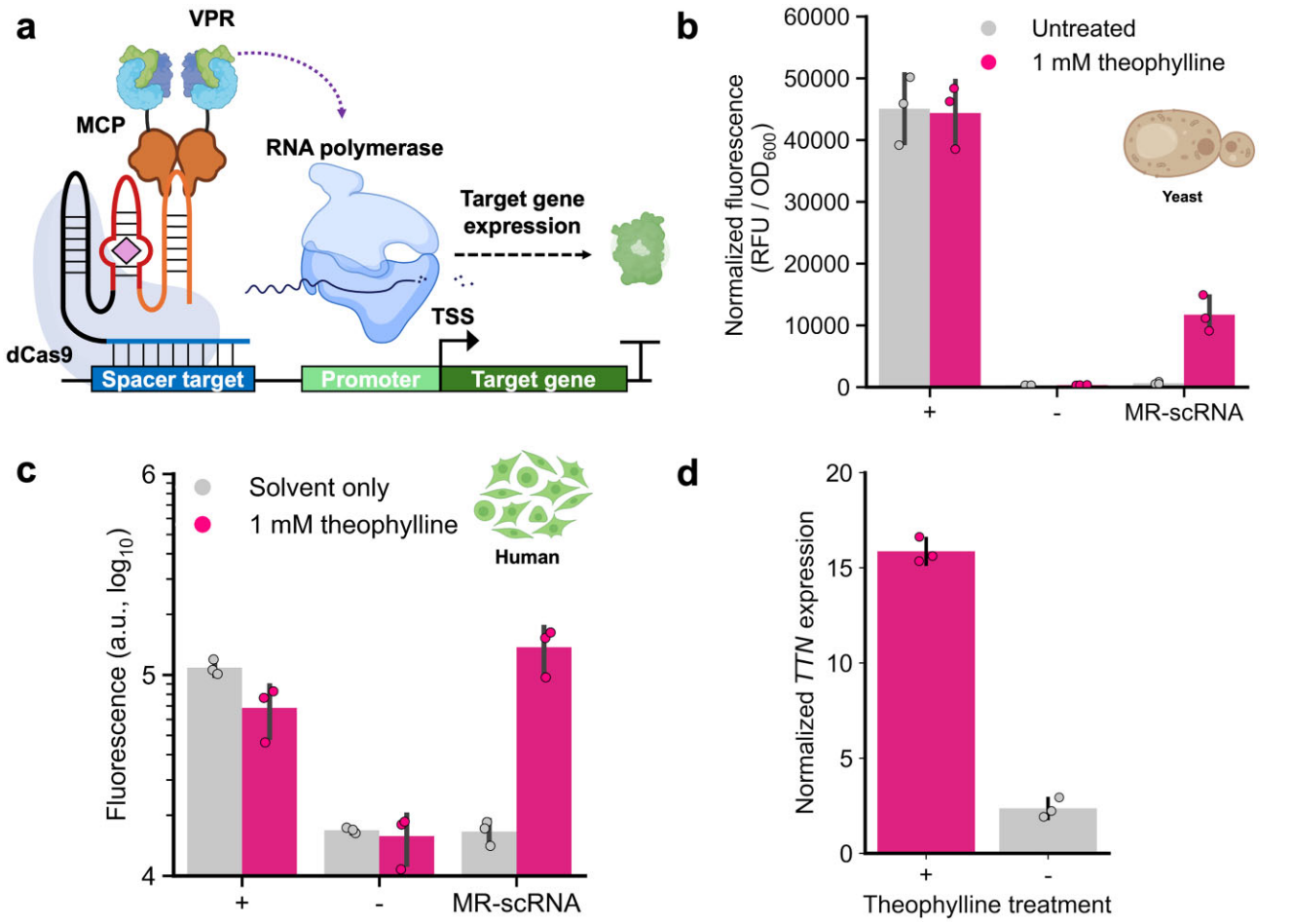

Figure 3. MR-scRNAs drive conditional gene activation in yeast and human cells. (**A**) Design schematic of the MR-scRNA system in yeast and human cells. (**B**) *Saccharomyces cerevisiae* cells with an integrated pTET07-Venus reporter and galactose-inducible CRISPRa machinery were transformed with an on-target scRNA (+), non-targeting scRNA (−), or theophylline-responsive scRNA (MR-scRNA). Yeast cells were induced with 0.01% w/v galactose and cultivated with or without theophylline. All values are mean ± s.d. of $n = 3$ biological replicates. (**C**) HEK239T pTRE3G-dscGFP cells were transfected with dCas9 and MCP-VPR expression plasmids as well as an scRNA (+), sgRNA (−), or theophylline-responsive scRNA (MR-scRNA). HEK293T cells were induced with either 1 mM theophylline or a solvent-only control 24 h after transfection. (**D**) HEK293T cells were transfected with dCas9 and MCP-VPR expression plasmids as well as MR-scRNA targeting TTN. HEK293T cells were induced with either 1 mM theophylline or a solvent-only control 24 h after transfection, and RNA was extracted 48 h after transfection. Gene expression was normalized to GAPDH mRNA levels within each sample and compared against cells transfected with a non-targeting MR-scRNA without theophylline stimulation. All values are mean ± s.d. of $n = 3$ biological replicates. Abbreviations: RFU, relative fluorescent units; OD_{600}, optical density at 600 nm; a.u., arbitrary units.

ditionally control the expression of endogenous genes. We transfected HEK293T cells with a plasmid expressing MR-scRNAs with a spacer targeting titin (TTN). As expected, we found expression of TTN was significantly elevated in cells treated with 1 mM theophylline compared to untreated cells (Fig. 3D).

The canonical NGG protospacer-adjacent motif (PAM) site requirement for DNA-binding limits the number of genes that can be regulated by CRISPRa [51]. Thus, we also explored whether MR-scRNAs would function similarly with alternative dCas9 variants with expanded PAM ranges, such as the engineered SpRY variant [52, 53]. Previous work has demonstrated that the dSpRY variant could activate a range of endogenous genes with noncanonical PAM sites [33, 54]. We detected similar levels of conditional gene activation using the MR-scRNA in conjunction with either dCas9 or dSpRY (Supplementary Fig. S9), which greatly expands the number of genes that can be targeted with the MR-scRNA system.

Dynamic metabolic regulation using MR-scRNAs responsive to native metabolite

We next sought to design an MR-scRNA that can sense and respond to a native metabolite. Tryptophan is a precursor for the biosynthesis of many natural products and medicinal compounds [2, 55–59], yet it is also an amino acid essential for protein synthesis and thus growth. Dynamic regulatory strategies that consider the concentrations of key branch point metabolites, such as tryptophan, offer improved product titers and yields [10, 11]. Thus, we created a tryptophan-responsive scRNA that can be used as a metabolic switch to transition between growth and production states when tryptophan levels are high (Fig. 4A).

Given the high hit rate from our initial screen for theophylline-responsive scRNAs, we generated a single tryptophan MR-scRNA by simply implementing the highest-ranked RNA switch from the *in vitro* screening for this metabolite into our scRNA [32]. We cultivated different *E. coli* strains expressing this new MR-scRNA design and the

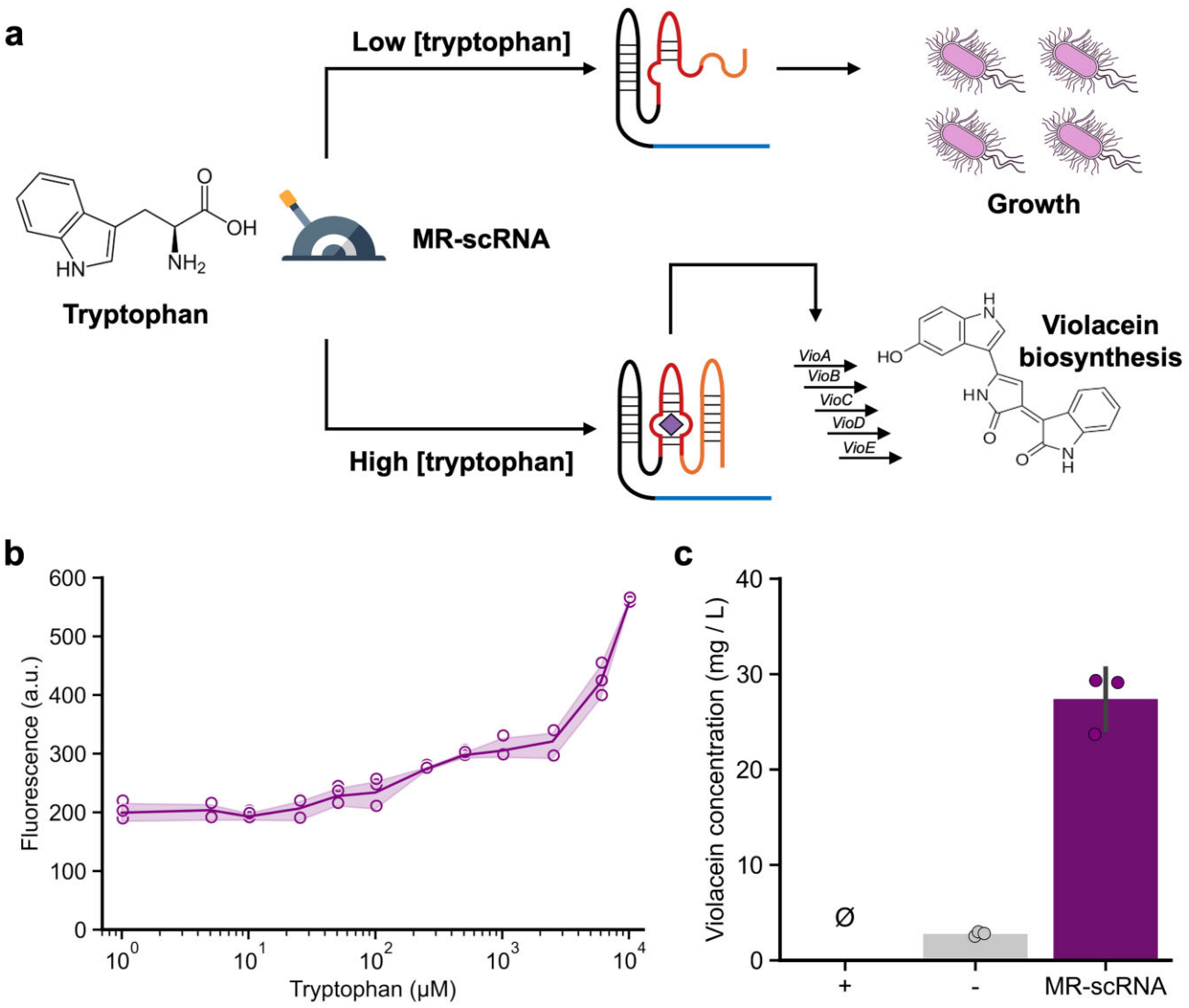

Figure 4. Dynamic regulation of biosynthesis pathway with tryptophan-responsive MR-scRNAs. (**A**) Design schematic illustrating the dynamic regulatory strategy used to conditionally activate the violacein biosynthesis pathway in response to concentrations of the upstream metabolite, tryptophan, that is required for both growth and biochemical production. (**B**) Dose–response curve of the tryptophan MR-scRNA in response to the target metabolite. (**C**) Violacein titer extracted from *E. coli* cells with the violacein biosynthesis pathway activated by an on-target scRNA (+), non-targeting scRNA (−), or a tryptophan-responsive scRNA (MR-scRNA). Abbreviations: Ø, not detected; a.u., arbitrary units.

proper controls in rich, defined media supplemented with or without tryptophan (Supplementary Fig. S10). As expected, only cells with the tryptophan MR-scRNA exhibited conditional gene activation. The tryptophan MR-scRNA appears leakier than the theophylline MR-scRNA, likely due to tryptophan synthesized by the growing cells. We observed dose-dependent behavior of the tryptophan MR-scRNA in response to its cognate ligand with a minimum detectable concentration of 250 μM and a maximum 2.8-fold response (Fig. 4B and Supplementary Fig. S11). We also ported the tryptophan MR-scRNA into yeast, which enabled a slight but significant response to tryptophan in this host (Supplementary Fig. S12) with higher levels of background expression likely induced by the tryptophan present within the media formulation required for this auxotrophic strain.

After validating our tryptophan-responsive MR-scRNA, we then sought to dynamically regulate violacein production. Violacein is a naturally occurring purple pigment with anti-microbial and anti-tumor properties synthesized in a five-enzyme cascade (VioABECD) from tryptophan [60]. We first attempted to use the theophylline-responsive MR-scRNA to conditionally activate expression of these five genes (Supplementary Fig. S13). We found that there was a slight but not statistically significant increase in violacein titers when these cells were treated with theophylline. However, the increase in violacein production is more pronounced on a per-cell basis due to a roughly two-fold reduction in biomass from the metabolic burden of background overexpression. We next utilized the tryptophan MR-scRNA to permit cells to self-regulate their expression of the violacein biosynthesis pathway when there is sufficient tryptophan available for both growth and production.

We compared violacein production in *E. coli* with either an on-target scRNA (constitutively high expression), an off-target scRNA (basal expression), or a tryptophan MR-scRNA (conditional expression) (Fig. 4C and Supplementary Fig. S14). The tryptophan MR-scRNA produced 9.9-fold greater violacein than the off-target scRNA control without any ap-

parent growth defects. Self-regulation with a tryptophan MR-scRNA proved useful, as this strategy led to 3.6-fold more violacein than the theophylline MR-scRNA despite the fact that the level of induced mRFP1 expression with the theophylline MR-scRNA was higher than with the tryptophan MR-scRNA. Interestingly, no detectable quantity of violacein was produced by cultures with the on-target scRNA in any of our experiments. We did observe purple colonies when these cells were initially transformed onto agar plates, but violacein production capacity was completely abolished in liquid media across each of our experiments. This, coupled with slower overall growth of these cultures, indicates an extreme metabolic burden placed on these cells by constitutive high expression of this multi-gene pathway. Overall, the design of MR-scRNAs responsive to branch point metabolites, such as tryptophan, that are essential for both growth and biochemical production provides a new dynamic regulatory strategy to achieve more effective biosynthesis.

Discussion

In this work, we present MR-scRNAs as a programmable and generalizable tool for metabolite-inducible CRISPR transcriptional activation. We demonstrated that MR-scRNAs are capable of functioning in three distinct species from across the tree of life and are thus likely to be portable to many other hosts. We were also able to demonstrate that MR-scRNAs responsive to alternative metabolites could be generated. Additionally, the utility of the MR-scRNA for dynamic metabolic engineering was demonstrated using a tryptophan-responsive MR-scRNA to enable cells to self-regulate precursor levels leading to more efficient cell growth and biosynthesis of violacein.

Our MR-scRNAs have comparable activation profiles to other ligand-inducible CRISPRa platforms in bacteria and yeast [19, 21, 29], with several potential benefits. First, modulation of gene regulation through a *cis*-acting RNA switch instead of conventional chemical-inducible dimerization (CID) domains, such as PYL1-ABI or GID1-GAI, minimizes the number of biological components that must be expressed, which reduces the burden imposed by the presence of the regulatory system. Furthermore, ligand-inducible CRISPRa systems that rely on CID are limited to the small number of available molecules that can be sensed with such pairings whereas the possible range of inputs that an MR-scRNA could possibly detect is significantly broader given that there are several hundred natural and synthetic RNA aptamers have already been identified [61]. It is important to note that small molecules with simple structures are targets that an RNA aptamer is unlikely to be generated for, and many existing RNA aptamers bind to proteins instead of metabolites [46, 61].

Our MR-scRNA builds upon other metabolite-responsive gRNA designs. Previous small-molecule-responsive sgRNA designs used an aptamer or aptazyme to regulate CRISPR activity to impede binding of the dCas9 to the sgRNA or to sequester the spacer sequence [28–31, 62]. A key advantage of our MR-scRNA design is preserving the native sgRNA–Cas9 interaction by shifting the regulatory control point to the effector recruitment motif instead of the Cas9-binding hairpin. Embedding the metabolite-sensing domain outside of the existing functional elements of the gRNA likely minimizes the impairment of dCas9-binding ability. For instance, a previous small-molecule-responsive sgRNA design for conditional CRISPRi regulation in bacteria that performed similarly to ours in bacteria (Supplementary Fig. S15) was non-functional in eukaryotes, which the authors speculated was due to their sgRNA's reduced affinity for the Cas9 protein [29]. To the best of our knowledge, our design is the first metabolite-responsive gRNA design functional in each of bacterial, yeast, and mammalian cells. Additionally, the fast and dynamic response behavior of the MR-scRNA is likely supported by modulating effector localization rather than dCas9-binding, given that dCas9 remains bound to the target DNA until replication [63]. Compared to other RNA regulatory systems, such as riboswitches or ribozymes [43, 64, 65], the MR-scRNA has an enhanced dynamic range and the ability to target both heterologous and endogenous genes without genetic reprogramming. Overall, the MR-scRNA is simple to design and repurpose for different applications while maintaining sufficient regulatory capacity.

Further optimization of the MR-scRNA system is needed to reduce basal activation in the unbound "off" state and improve gene activation in the ligand-bound "on" state. Depending on the exact MR-scRNA variant and application, background gene expression varied between ∼1- to ∼10-fold that of a non-targeting control. Careful balancing of the ratio of MR-scRNA to the MCP-activator could reduce non-specific binding of these two components, as the 'off' state K_D of the theophylline and tryptophan MR-scRNAs for MCP is only ∼500 nM [32]. The lower maximum output of an activated MR-scRNA compared to a static scRNA is likely explained by the reduced affinity of the "on" state RNA switches, with the K_D of the RNA switches for MCP being roughly 25-fold higher than that of the static MS2 aptamer [32, 66]. However, as demonstrated during violacein biosynthesis, there are benefits in intermediate levels of gene activation that are initiated under certain conditions. Despite directly porting the bacterial MR-scRNA design into mammalian cells, we found that MR-scRNA were most successful in human cells relative to our experiments in bacteria and yeast. In mammalian cells, the MR-scRNA has a maximal output matching that of the conventional scRNA and no leakiness compared to an untransfected control. This result may be attributed to the modest performance of scRNA designs with only a single MCP-binding domain, as multiple MS2 aptamers are required to achieve high levels of gene activation in human cells [18]. Similar to previous work, the incorporation of multiple RNA switches into the scRNA could improve activation through multivalent recruitment of transcriptional activators [18, 50, 67].

Our MR-scRNA design exploits the excellent RNA switches generated by the online game, *Eterna*, and the high-throughput screening performed by the Das and Greenleaf labs [32, 68, 69]. Designs solicited by citizen scientists playing the *Eterna* game are highly efficient binders of the target ligand, whether that is a small molecule, RNA, or protein, and often perform better than expert- or computationally-designed alternatives [32, 70, 71]. These RNA switches were not previously characterized for intracellular activity and were surprisingly robust in our testing (7 functional variants out of 11 tested variants) despite significant differences between the original screening conditions and the intracellular environment in which they were tested here. This RNA design space offers opportunities for the development of MR-scRNA responsive to other metabolites. However, a limitation of using

RNA switches developed from *Eterna* for our MR-scRNAs is our reliance on grafting *in vitro* characterized components onto an sgRNA. RNA secondary structure interactions have a significant impact on the final structure and thus function of an RNA molecule [72, 73]. This is especially true in the design of effective sgRNA that must interface with multiple biological components (dCas9, MCP, and target DNA) [74] simultaneously while maintaining the correct spatial orientation required for recruitment of the RNA polymerase by the effector [14, 15, 21]. Thus, due to the complex and dynamic secondary structure of the MR-scRNA, larger libraries of distinct designs are needed to better understand these limitations and predict RNA switch performance a priori by expanding upon existing thermodynamic and kinetic gRNA performance models [74] using spatial orientation and distance identified by structural modeling of the RNA-protein complexes [75, 76]. The creation of *Eterna* challenges that are specific to a combined sgRNA-RNA switch design coupled with intracellular library-based CRISPRa screening methods [77] could lead to the development of improved MR-scRNAs that are responsive to alternative ligands or bind to different protein effectors for orthogonal gene modulation.

In conclusion, MR-scRNAs offer a promising platform for metabolite-responsive transcriptional control. With minimal modifications, we demonstrate that MR-scRNAs can be adapted to respond to new inputs or function in different environmental contexts while maintaining the existing functionality of CRISPR-based transcriptional regulators. In addition to acting as dynamic regulators, MR-scRNAs responsive to products or pathway intermediates could be used as a biosensors to screen libraries for pathway optimization or enzyme engineering. MR-scRNAs also expand the number of orthogonal inputs available for regulation of gene circuits in mammalian synthetic biology. Overall, we believe that the favorable ligand-responsive characteristics and the versatility displayed by our MR-scRNAs offer a broadly useful tool for conditional modulation of gene expression.

Acknowledgements

The authors thank J. Nicosia and H. Alam for assistance with plasmid construction. Portions of several figures were created in BioRender [78].

Author contributions: Anthony M. Stohr (Conceptualization [lead], Data curation [lead], Formal analysis [lead], Methodology [lead], Writing – original draft [equal], Helena Hansen (Data curation [supporting], Blake Richards (Data curation [supporting], Hayeon Park (Data curation [supporting], Antonio G. Goncalves (Data curation [supporting], Ayushi Agrawal (Data curation [supporting], Mark Blenner (Conceptualization [lead], Formal analysis [equal], Funding acquisition [lead], Investigation [equal], Methodology [equal], Project administration [equal], Supervision [equal], Writing – original draft [equal], and Wilfred Chen (Conceptualization [equal], Formal analysis [equal], Funding acquisition [lead], Investigation [equal], Methodology [equal], Project administration [equal], Supervision [equal], Writing – original draft [equal]

Supplementary data

Supplementary data is available at NAR online.

Conflict of interest

None declared.

Funding

This work was supported in part by a grant from the National Science Foundation (MCB2317398 awarded to W.C.) and the U.S. National Institutes of Health (GM133803 awarded to M.B.). A.M.S. was supported in part by the U.S. Department of Defense through the NDSEG Fellowship Program and the U.S. Department of Education through a GAANN Fellowship Program (P200A210065).

Data availability

All data supporting the findings of this study are available within the figures and the Supplementary data. All source data and custom analysis scripts are available with this publication. Plasmids used in this study are available from Addgene upon publication.

References

1. Keasling JD. Manufacturing molecules through metabolic engineering. *Science* 2010;330:1355–8. https://doi.org/10.1126/science.1193990
2. Zhang J, Hansen LG, Gudich O *et al.* A microbial supply chain for production of the anti-cancer drug vinblastine. *Nature* 2022;609:341–7. https://doi.org/10.1038/s41586-022-05157-3
3. Ganesan V, Monteiro L, Pedada D *et al.* High-efficiency multiplexed cytosine base editors for natural product synthesis in *Yarrowia lipolytica*. *ACS Synth Biol* 2023;12:3082–91. https://doi.org/10.1021/acssynbio.3c00435
4. Liu Y, Zhao X, Gan F *et al.* Complete biosynthesis of QS-21 in engineered yeast. *Nature* 2024;629:937–44. https://doi.org/10.1038/s41586-024-07345-9
5. Alper H, Fischer C, Nevoigt E *et al.* Tuning genetic control through promoter engineering. *Proc Natl Acad Sci USA* 2005;102:12678–83. https://doi.org/10.1073/pnas.0504604102
6. Ghodasara A, Voigt CA. Balancing gene expression without library construction via a reusable sRNA pool. *Nucleic Acids Res* 2017;45:8116–27. https://doi.org/10.1093/nar/gkx530
7. Jones JA, Vernacchio VR, Lachance DM *et al.* ePathOptimize: a combinatorial approach for transcriptional balancing of metabolic pathways. *Sci Rep* 2015;5:11301. https://doi.org/10.1038/srep11301
8. Yuan S, Xu C, Jin M *et al.* Stress-driven dynamic regulation of multiple genes to reduce accumulation of toxic aldehydes. *Metab Eng* 2025;90:129–40. https://doi.org/10.1016/j.ymben.2025.03.009
9. Solomon KV, Sanders TM, Prather KLJ. A dynamic metabolite valve for the control of central carbon metabolism. *Metab Eng* 2012;14:661–71. https://doi.org/10.1016/j.ymben.2012.08.006
10. Ni C, Dinh CV, Prather KLJ. Dynamic control of metabolism. *Annu Rev Chem Biomol Eng* 2021;12:519–41. https://doi.org/10.1146/annurev-chembioeng-091720-125738
11. Venayak N, Anesiadis N, Cluett WR *et al.* Engineering metabolism through dynamic control. *Curr Opin Biotechnol* 2015;34:142–52. https://doi.org/10.1016/j.copbio.2014.12.022
12. Brockman IM, Prather KLJ. Dynamic metabolic engineering: new strategies for developing responsive cell factories. *Biotechnol J* 2015;10:1360–9. https://doi.org/10.1002/biot.201400422
13. Gilbert LA, Larson MH, Morsut L *et al.* CRISPR-mediated modular RNA-guided regulation of transcription in eukaryotes. *Cell* 2013;154:442–51. https://doi.org/10.1016/j.cell.2013.06.044

14. Dong C, Fontana J, Patel A *et al.* Synthetic CRISPR–Cas gene activators for transcriptional reprogramming in bacteria. *Nat Commun* 2018;9:2489. https://doi.org/10.1038/s41467-018-04901-6
15. Fontana J, Dong C, Kiattisewee C *et al.* Effective CRISPRa-mediated control of gene expression in bacteria must overcome strict target site requirements. *Nat Commun* 2020;11:1618. https://doi.org/10.1038/s41467-020-15454-y
16. Villegas Kcam MC, Tsong AJ, Chappell J. Rational engineering of a modular bacterial CRISPR–Cas activation platform with expanded target range. *Nucleic Acids Res* 2021;49:4793–802. https://doi.org/10.1093/nar/gkab211
17. Kiattisewee C, Dong C, Fontana J *et al.* Portable bacterial CRISPR transcriptional activation enables metabolic engineering in *Pseudomonas putida*. *Metab Eng* 2021;66:283–95. https://doi.org/10.1016/j.ymben.2021.04.002
18. Zalatan JG, Lee ME, Almeida R *et al.* Engineering complex synthetic transcriptional programs with CRISPR RNA scaffolds. *Cell* 2015;160:339–50. https://doi.org/10.1016/j.cell.2014.11.052
19. Cunningham-Bryant D, Sun J, Fernandez B *et al.* CRISPR–Cas-mediated chemical control of transcriptional dynamics in yeast *Chembiochem* 2019;20:1519–23.
20. Gao Y, Xiong X, Wong S *et al.* Complex transcriptional modulation with orthogonal and inducible dCas9 regulators. *Nat Methods* 2016;13:1043–9. https://doi.org/10.1038/nmeth.4042
21. Burbano DA, Cardiff RAL, Tickman BI *et al.* Engineering activatable promoters for scalable and multi-input CRISPRa/i circuits. *Proc Natl Acad Sci USA* 2023;120:e2220358120. https://doi.org/10.1073/pnas.2220358120
22. Tague N, Coriano-Ortiz C, Sheets MB *et al.* Light inducible protein degradation in *E. coli* with the LOVdeg tag. *eLife* 2024;12:RP87303. https://doi.org/10.7554/eLife.87303.3
23. Stohr AM, Ma D, Chen W *et al.* Engineering conditional protein-protein interactions for dynamic cellular control. *Biotechnol Adv* 2024;77:108457. https://doi.org/10.1016/j.biotechadv.2024.108457
24. Dey SK, Filonov GS, Olarerin-George AO *et al.* Repurposing an adenine riboswitch into a fluorogenic imaging and sensing tag. *Nat Chem Biol* 2021;18:180–90. https://doi.org/10.1038/s41589-021-00925-0
25. Samuelian JS, Gremminger TJ, Song Z *et al.* An RNA aptamer that shifts the reduction potential of metabolic cofactors. *Nat Chem Biol* 2022;18:1263–9. https://doi.org/10.1038/s41589-022-01121-4
26. White N, Sadeeshkumar H, Sun A *et al.* Na^+ riboswitches regulate genes for diverse physiological processes in bacteria. *Nat Chem Biol* 2022;18:878–85. https://doi.org/10.1038/s41589-022-01086-4
27. Vezeau GE, Gadila LR, Salis HM. Automated design of protein-binding riboswitches for sensing human biomarkers in a cell-free expression system. *Nat Commun* 2023;14:2416. https://doi.org/10.1038/s41467-023-38098-0
28. Tang W, Hu JH, Liu DR. Aptazyme-embedded guide RNAs enable ligand-responsive genome editing and transcriptional activation. *Nat Commun* 2017;8:15939. https://doi.org/10.1038/ncomms15939
29. Kundert K, Lucas JE, Watters KE *et al.* Controlling CRISPR–Cas9 with ligand-activated and ligand-deactivated sgRNAs. *Nat Commun* 2019;10:2127. https://doi.org/10.1038/s41467-019-09985-2
30. Liu X-H, Li B-R, Ying Z-M *et al.* Small-molecule-mediated split-aptamer assembly for inducible CRISPR–dCas9 transcription activation. *ACS Chem Biol* 2022;17:1769–77. https://doi.org/10.1021/acschembio.2c00101
31. Liu Y, Zhan Y, Chen Z *et al.* Directing cellular information flow via CRISPR signal conductors. *Nat Methods* 2016;13:938–44. https://doi.org/10.1038/nmeth.3994
32. Andreasson JOL, Gotrik MR, Wu MJ *et al.* Crowdsourced RNA design discovers diverse, reversible, efficient, self-contained molecular switches. *Proc Natl Acad Sci USA* 2022;119:e2112979119. https://doi.org/10.1073/pnas.2112979119
33. Kiattisewee C, Karanjia AV, Legut M *et al.* Expanding the scope of bacterial CRISPR activation with PAM-flexible dCas9 variants. *ACS Synth Biol* 2022;11:4103–12. https://doi.org/10.1021/acssynbio.2c00405
34. Cress BF, Jones JA, Kim DC *et al.* Rapid generation of CRISPR/dCas9-regulated, orthogonally repressible hybrid T7-lac promoters for modular, tuneable control of metabolic pathway fluxes in Escherichia coli. *Nucleic Acids Res* 2016;44:4472–85. https://doi.org/10.1093/nar/gkw231
35. Xu X, Chemparathy A, Zeng L *et al.* Engineered miniature CRISPR–Cas system for mammalian genome regulation and editing. *Mol Cell* 2021;81:4333–45. https://doi.org/10.1016/j.molcel.2021.08.008
36. Livak KJ, Schmittgen TD. Analysis of relative gene expression data using real-time quantitative PCR and the $2-\Delta\Delta CT$ method. *Methods* 2001;25:402–8. https://doi.org/10.1006/meth.2001.1262
37. Wrist A, Sun W, Summers RM. The theophylline aptamer: 25 years as an important tool in cellular engineering research. *ACS Synth Biol* 2020;9:682–97. https://doi.org/10.1021/acssynbio.9b00475
38. Kawamukai M, Murao K, Utsumi R *et al.* Cell filamentation in an *Escherichia coli* K-12 fic mutant caused by theophylline or an adenylate cyclase gene (cya)-containing plasmid. *FEMS Microbiol Lett* 1986;34:117–20. https://doi.org/10.1111/j.1574-6968.1986.tb01360.x
39. Desai SK, Gallivan JP. Genetic screens and selections for small molecules based on a synthetic riboswitch that activates protein translation. *J Am Chem Soc* 2004;126:13247–54. https://doi.org/10.1021/ja048634j
40. Rankin CJ, Fuller EN, Hamor KH *et al.* A simple fluorescent biosensor for theophylline based on its RNA aptamer. *Nucleosides Nucleotides Nucleic Acids* 2006;25:1407–24. https://doi.org/10.1080/15257770600919084
41. Balleza E, Kim JM, Cluzel P. Systematic characterization of maturation time of fluorescent proteins in living cells. *Nat Methods* 2018;15:47–51. https://doi.org/10.1038/nmeth.4509
42. Chavez A, Scheiman J, Vora S *et al.* Highly efficient Cas9-mediated transcriptional programming. *Nat Methods* 2015;12:326–8. https://doi.org/10.1038/nmeth.3312
43. Wang X, Fang C, Wang Y *et al.* Systematic comparison and rational design of theophylline riboswitches for effective gene repression. *Microbiol Spectr* 2023;11:e02752–22.
44. Wu L, Liu Z, Liu Y. Thermal adaptation of structural dynamics and regulatory function of adenine riboswitch. *RNA Biol* 2021;18:2007–15. https://doi.org/10.1080/15476286.2021.1886755
45. Fürtig B, Oberhauser EM, Zetzsche H *et al.* Refolding through a linear transition state enables fast temperature adaptation of a translational riboswitch. *Biochemistry* 2020;59:1081–6. https://doi.org/10.1021/acs.biochem.9b01044
46. Carothers JM, Goler JA, Kapoor Y *et al.* Selecting RNA aptamers for synthetic biology: investigating magnesium dependence and predicting binding affinity. *Nucleic Acids Res* 2010;38:2736–47. https://doi.org/10.1093/nar/gkq082
47. Roy S, Hennelly SP, Lammert H *et al.* Magnesium controls aptamer-expression platform switching in the SAM-I riboswitch. *Nucleic Acids Res* 2019;47:3158–70. https://doi.org/10.1093/nar/gky1311
48. Grubbs RD. Intracellular magnesium and magnesium buffering. *Biometals* 2002;15:251–9. https://doi.org/10.1023/A:1016026831789
49. Romani AMP. Magnesium homeostasis in mammalian cells. In Banci L (ed.), *Metallomics and the Cell*. Netherlands, Dordrecht: Springer, 2013, 69–118.
50. Konermann S, Brigham MD, Trevino AE *et al.* Genome-scale transcriptional activation by an engineered CRISPR–Cas9

complex. *Nature* 2015;517:583–8. https://doi.org/10.1038/nature14136
51. Jiang F, Doudna JA. CRISPR–Cas9 structures and mechanisms. *Annu Rev Biophys* 2017;46:505–29. https://doi.org/10.1146/annurev-biophys-062215-010822
52. Walton RT, Christie KA, Whittaker MN *et al.* Unconstrained genome targeting with near-PAMless engineered CRISPR–Cas9 variants. *Science* 2020;368:290–6. https://doi.org/10.1126/science.aba8853
53. Hibshman GN, Bravo JPK, Hooper MM *et al.* Unraveling the mechanisms of PAMless DNA interrogation by SpRY-Cas9. *Nat Commun* 2024;15:3663. https://doi.org/10.1038/s41467-024-47830-3
54. Klanschnig M, Cserjan-Puschmann M, Striedner G *et al.* CRISPRactivation-SMS, a message for PAM sequence independent gene up-regulation in *Escherichia coli*. *Nucleic Acids Res* 2022;50:10772–84. https://doi.org/10.1093/nar/gkac804
55. Ishihara A, Matsuda F, Miyagawa H *et al.* Metabolomics for metabolically manipulated plants: effects of tryptophan overproduction. *Metabolomics* 2007;3:319–34. https://doi.org/10.1007/s11306-007-0072-4
56. Brown S, Clastre M, Courdavault V *et al. De novo* production of the plant-derived alkaloid strictosidine in yeast. *Proc Natl Acad Sci USA* 2015;112:3205–10. https://doi.org/10.1073/pnas.1423555112
57. Reed KB, Brooks SM, Wells J *et al.* A modular and synthetic biosynthesis platform for de novo production of diverse halogenated tryptophan-derived molecules. *Nat Commun* 2024;15:3188. https://doi.org/10.1038/s41467-024-47387-1
58. Mavros CF, Bongers M, Neergaard FBF *et al.* Bacteria engineered to produce serotonin modulate host intestinal physiology. *ACS Synth Biol* 2024;13:4002–14. https://doi.org/10.1021/acssynbio.4c00453
59. Mitkas AA, Valverde M, Chen W. Dynamic modulation of enzyme activity by synthetic CRISPR–Cas6 endonucleases. *Nat Chem Biol* 2022;18:492–500. https://doi.org/10.1038/s41589-022-01005-7
60. Durán N, Justo GZ, Durán M *et al.* Advances in *Chromobacterium violaceum* and properties of violacein-Its main secondary metabolite: a review. *Biotechnol Adv* 2016;34:1030–45. https://doi.org/10.1016/j.biotechadv.2016.06.003
61. Askari A, Kota S, Ferrell H *et al.* UTexas Aptamer Database: the collection and long-term preservation of aptamer sequence information. *Nucleic Acids Res* 2024;52:D351–9. https://doi.org/10.1093/nar/gkad959
62. Iwasaki RS, Ozdilek BA, Garst AD *et al.* Small molecule regulated sgRNAs enable control of genome editing in E. coli by Cas9. *Nat Commun* 2020;11:1394. https://doi.org/10.1038/s41467-020-15226-8
63. Jones DL, Leroy P, Unoson C *et al.* Kinetics of dCas9 target search in *Escherichia coli*. *Science* 2017;357:1420–4. https://doi.org/10.1126/science.aah7084
64. Jang S, Jung GY. Systematic optimization of L-tryptophan riboswitches for efficient monitoring of the metabolite in *Escherichia coli*. *Biotechnol Bioeng* 2018;115:266–71. https://doi.org/10.1002/bit.26448
65. Townshend B, Xiang JS, Manzanarez G *et al.* A multiplexed, automated evolution pipeline enables scalable discovery and characterization of biosensors. *Nat Commun* 2021;12:1437. https://doi.org/10.1038/s41467-021-21716-0
66. Tutucci E, Vera M, Biswas J *et al.* An improved MS2 system for accurate reporting of the mRNA life cycle. *Nat Methods* 2018;15:81–9. https://doi.org/10.1038/nmeth.4502
67. Chen R, Shi X, Yao X *et al.* Specific multivalent molecules boost CRISPR-mediated transcriptional activation. *Nat Commun* 2024;15:7222. https://doi.org/10.1038/s41467-024-51694-y
68. Lee J, Kladwang W, Lee M *et al.* RNA design rules from a massive open laboratory. *Proc Natl Acad Sci USA* 2014;111:2122–7. https://doi.org/10.1073/pnas.1313039111
69. Buenrostro JD, Araya CL, Chircus LM *et al.* Quantitative analysis of RNA–protein interactions on a massively parallel array reveals biophysical and evolutionary landscapes. *Nat Biotechnol* 2014;32:562–8. https://doi.org/10.1038/nbt.2880
70. Choe C, Andreasson JOL, Melaine F *et al.* Compact RNA sensors for increasingly complex functions of multiple inputs. *Nat Chem* 2025. https://doi.org/10.1038/s41557-025-01907-8
71. Wu MJ, Andreasson JOL, Kladwang W *et al.* Automated design of diverse stand-alone riboswitches. *ACS Synth Biol* 2019;8:1838–46. https://doi.org/10.1021/acssynbio.9b00142
72. Townshend RJL, Eismann S, Watkins AM *et al.* Geometric deep learning of RNA structure. *Science* 2021;373:1047–51.
73. Wayment-Steele HK, Kladwang W, Strom AI *et al.* RNA secondary structure packages evaluated and improved by high-throughput experiments. *Nat Methods* 2022;19:1234–42. https://doi.org/10.1038/s41592-022-01605-0
74. Fontana J, Sparkman-Yager D, Faulkner I *et al.* Guide RNA structure design enables combinatorial CRISPRa programs for biosynthetic profiling. *Nat Commun* 2024;15:6341. https://doi.org/10.1038/s41467-024-50528-1
75. Abramson J, Adler J, Dunger J *et al.* Accurate structure prediction of biomolecular interactions with AlphaFold 3. *Nature* 2024;630:493–500. https://doi.org/10.1038/s41586-024-07487-w
76. Baek M, McHugh R, Anishchenko I *et al.* Accurate prediction of protein–nucleic acid complexes using RoseTTAFoldNA. *Nat Methods* 2024;21:117–21. https://doi.org/10.1038/s41592-023-02086-5
77. Su-Tobon Q, Fan J, Goldstein M *et al.* CRISPR-hybrid: a CRISPR-mediated intracellular directed evolution platform for RNA aptamers. *Nat Commun* 2025;16:595. https://doi.org/10.1038/s41467-025-55957-0
78. Stohr A. 2025. https://BioRender.com/7pe9tp7

Received: July 27, 2025. **Revised:** October 16, 2025. **Accepted:** October 17, 2025